ISTITUTO NAZIONALE DI FISICA NUCLEARE
Laboratori Nazionali di Frascati

LNF-81/22

M. Basile, G. Cara Romeo, L. Cifarelli, G. D'Ali, P. Di Cesare, P. Giusti, T. Massam, F. Palmonari, G. Sartorelli, G. Valenti, A. Contin, F. Favale, A. Zichichi and B. Esposito: A LARGE AREA TIME-OF-FLIGHT SYSTEM FOR A COLLIDING BEAM MACHINE

Estratto da:
Nuclear Instr. and Meth. 179, 477 (1981)

Servizio Documentazione
dei Laboratori Nazionali di Frascati

Nuclear Instruments and Methods 179 (1981) 477–485

A LARGE-AREA TIME-OF-FLIGHT SYSTEM FOR A COLLIDING BEAM MACHINE

A. BASILE
Istituto di Fisica, Università di Bologna, Bologna, Italy

G. CARA ROMEO, L. CIFARELLI, G. D'ALI, P. Di CESARE, P. GIUSTI, T. MASSAM, F. PALMONARI, G. SARTORELLI, G. VALENTI
Istituto Nazionale di Fisica Nucleare, Sezione di Bologna, Italy

M. CONTIN, L. FAVALE, A. ZICHICHI
CERN, Geneva, Switzerland

and

R. ESPOSITO
Istituto Nazionale di Fisica Nucleare, Laboratori Nazionali di Frascati, Frascati, Italy

Received 16 July 1980

We describe the performance of a large solid-angle (2 sr) time-of-flight system used in conjunction with the Split Field Magnet spectrometer of the CERN Intersecting Storage Rings (ISR). The system consists of a hodoscope of 67 scintillator counters, at a distance of about 5 m from the beam intersection. The ISR being a coasting beam machine, contrary to the tightly bunched e^+e^- machines, the event time is unknown and therefore a special analysis procedure for particle identification is required.

We illustrate a powerful statistical method which allows the identification, with more than 90% efficiency, of pions up to about 1 GeV/c, kaons up to about 1.4 GeV/c, and protons up to about 2 GeV/c.

1. Introduction

In many colliding beam machines now in operation, a large fraction of the particles produced turns out to be of low momentum, say below 1.5 GeV/c. This suggests that the time-of-flight (TOF) technique is a powerful particle identification method. When the interaction time is not known with sufficient accuracy (i.e. from the machine radio-frequency), the standard TOF technique requires the measurement of the difference between the traversal times of the same particle across two scintillator counters separated by several metres. This requirement is in conflict with the need to cover a large solid angle, particularly when, as is often the case, the operation of scintillator counters (i.e. photomultipliers) near the interaction region is unpractical due to the presence of a strong magnetic field.

In the following we will describe a statistical method that has been implemented to identify particles produced in proton–proton interactions at the Split Field Magnet (SFM) facility of the CERN Intersecting Storage Rings (ISR), using a large solid-angle (2 sr) TOF system for the time measurement, and the SFM wire chambers' detector for the geometrical reconstruction and the momentum measurement (see fig. 1).

It is not the aim of this paper to describe the construction details or the characteristics of the associated electronics of such a system of counters. It is sufficient to point out that it consists of 67 scintillator counters ($2 \times 40 \times 225$ cm^3) viewed by one photomultiplier at each extremity [1].

2. Description of the method

2.1. Definition of the variables

Let us consider the schematic counter arrangement shown in fig. 2, and a typical event consisting of n

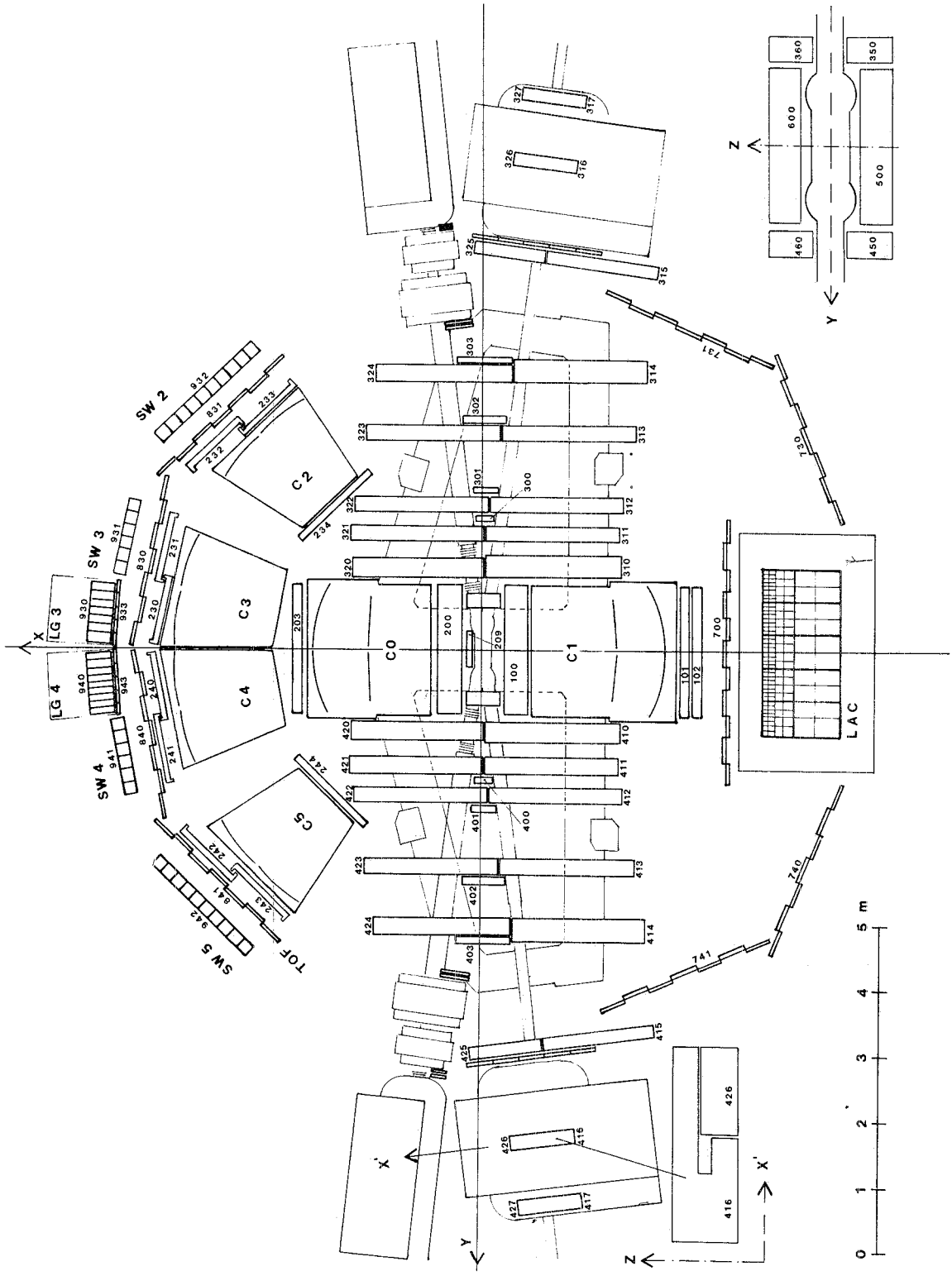

Fig. 1. Top view of R415 experimental apparatus used at the SFM facility of the CERN ISR: SW = sandwich-type electromagnetic shower detector; LG = lead-glass type electromagnetic shower detector; C = Cherenkov counter; LAC = liquid-argon calorimeter; TOF = time-of-flight counters.

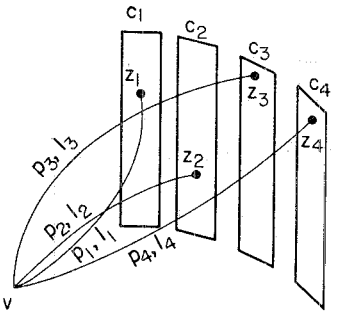

Fig. 2. A schematic view of a typical n-track event: C = time-of-flight counters; V = interaction vertex.

tracks hitting counters $C_1, C_2, ..., C_n$; $l_1, l_2, ..., l_n$ are the lengths of the trajectories from the common vertex V to the impact points $Z_1, Z_2, ..., Z_n$; and $p_1, p_2, ..., p_n$ are the relative momenta. (All these quantities are given by the reconstruction program, and will be considered as known.) The encoding electronics, shown in fig. 3 for one counter, records on the time-to-digital converter (TDC) the time difference between a "start" signal t_s, independently provided (in our case, by the trigger logic) and individual "stop" signals (two) for each counter hit. If we call this time interval $T_i^{U/D}$, where i refers to the counter as well as to the track index, and U/D refers to the two photomultipliers of counter i (symbolically called "up" and "down"), we can write:

$$T_i^{U/D} = (t_i^{U/D} + s_i^{U/D} + D_i^{U/D}) - (t_s + DS_i^{U/D}), \quad (1)$$

where:

t_s and $t_i^{U/D}$ are time intervals measured with

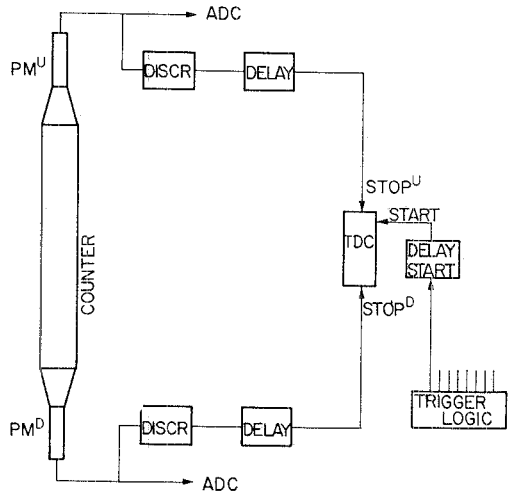

Fig. 3. Electronics diagram associated to each time-of-flight counter: DISCR = discriminator; PM = photomultiplier.

respect to the proton–proton interaction time, assumed to be $t_0 = 0$; t_s is the time needed by the trigger logic to accept the event, while $t_i^{U/D}$ is equal to the sum of the particle flight time from the interaction vertex to counter C_i and of the propagation time of the light in the scintillator counter from the impact point to the photomultiplier;

$D_i^{U/D}$ is the total delay of the electronic transmission line relative to photomultiplier $C_i^{U/D}$;

$s_i^{U/D}$ is the delay introduced by slewing effect in the discriminator of the $C_i^{U/D}$ signal; such a delay is in general a function of the number of photons seen by the photomultiplier, i.e. of the pulse height recorded by the analog-to-digital converter (ADC);

$DS_i^{U/D}$ is an extra delay of the "start" signal specific to the counter $C_i^{U/D}$ TDC. We can express the quantity $t_i^{U/D}$, appearing in eq. (1), as follows:

$$t_i^{U/D} = (l_i/c\beta_i) + z_i^{U/D}/v_i, \quad (2)$$

where l_i is the particle trajectory length, c is the speed of light in vacuum, β_i is the velocity of such a particle, $z_i^{U/D}$ is the distance of the impact point Z_i from the photomultiplier U/D, and v_i is the speed of light inside the scintillator counter C_i. Using eq. (2), expression (1) becomes

$$T_i^{U/D} = (l_i/c\beta_i) + (z_i^{U/D}/v_i) + d_i^{U/D} + s_i^{U/D} - t_s, \quad (3)$$

where $d_i^{U/D} = D_i^{U/D} - DS_i^{U/D}$ is a delay constant. Let us also define, for each counter, the following average time:

$$T_i = (T_i^U + T_i^D)/2 = (l_i/c\beta_i) + (L_i/2v_i) + d_i + s_i - t_s, \quad (4)$$

where $L_i = z_i^U + z_i^D$ is the counter length, $s_i = (s_i^U + s_i^D)/2$, and $d_i = (d_i^U + d_i^D)/2$. As can be seen, the quantity T_i is independent of the track impact point along the counter. Since the slewing corrections can be determined and applied, we can include the s_i term in T_i and write:

$$T_i = (l_i/c\beta_i) + D_i - t_s, \quad (5)$$

where we have defined a constant $D_i = d_i + (L_i/2v_i)$ which is specific to each channel (scintillator counter, photomultiplier, associated electronics, and transmission line). A way of determining these constants is described below.

In expression (5), the time t_s changes from event to event and is unknown. In the case, however, where at least two tracks are present in the apparatus –

which is not a severe requirement for the high multiplicity pp final states – we can define quantities, relating pairs of tracks and being independent of the event start-time. Namely, we can express the time relation between two counters, say i and j, as:

$$\Delta T_{ij} = T_i - T_j = [(l_i/c\beta_i) - (l_j/c\beta_j)] + (D_i - D_j) . \quad (6)$$

In this expression the left-hand side is measured. On the right-hand side, let us call $F_{ij} = D_i - D_j$ the constant relating counters i and j. If particles i and j are relativistic, we can assume $\beta_i \simeq \beta_j \simeq 1$ and determine

$$F_{ij} = (T_i - T_j) - (l_i - l_j)/c .$$

The most probable values of the F_{ij} distributions, obtained in this way with relativistic particles, have been determined for each pair of counters and used in the analysis.

The statistical method that we will describe in the following is based on the exclusive use of the quantities (6). The constants D_i will therefore always appear in the form $(D_i - D_j)$. Because of this, our system of n counters is completely characterized by the knowledge of $(n-1)$ constants F_{ij}. Notice that only $(n-1)$ elements out of n^2 of F_{ij} are independent and need to be determined, owing to the conditions

$$F_{ii} = 0 , \quad F_{ij} = -F_{ji} , \quad F_{ij} + F_{jk} = F_{ik} .$$

2.2. General solution for n-track events

Let us consider an event with $n \geqslant 2$ tracks. Expression (5) can be rewritten as

$$T_i = (l_i/c\beta_i) - g_a - F_{ai} , \quad (7)$$

where $g_a = t_s - D_a$ and $F_{ai} = D_a - D_i$ (with $F_{aa} = 0$). The index a, relative to any of the counters, is arbitrarily chosen. The quantity g_a is in fact, apart from a constant, the event start-time.

The system of n equations such as eq. (7), containing $(n+1)$ unknowns $\beta_1, \beta_2, \ldots, \beta_n$ and g_a, cannot give a unique solution. If, however, we require that the velocity

$$\beta_i = p_i/(m_i^2 + p_i^2)^{1/2}$$

is not a continuous variable but can assume only three values [$\beta(\pi)$, $\beta(K)$, and $\beta(p)$, obtained by attributing to the particle either the pion, or the kaon, or the proton mass], then, by assigning a mass configuration to the n particles of the event, we can request a "best fit" condition and derive the most probable mass configuration out of the possible $N = 3^n$.

For each event mass configuration $\mathcal{C}$, we can derive from each track i a start-time value $(g_a)_i$, as:

$$(g_a)_{i,\mathcal{C}} = [l_i/c(\beta_i)_{\mathcal{C}}] - T_i - F_{ai} , \quad (8)$$

and therefore compute the weighted average

$$\langle g_a \rangle_{\mathcal{C}} = \sum_{i=1}^{n} [(g_a)_{i,\mathcal{C}}/e_i^2] / \sum_{i=1}^{n} (1/e_i^2) , \quad (9)$$

where

$$e_i = [e_{T_i}^2 + (l_i/c\beta_i^2)^2 e_{\beta_i}^2 + (1/c\beta_i)^2 e_{l_i}^2 + e_{F_{ai}}^2]^{1/2} \quad (10)$$

is the error on g_a determination by means of track i, which is a function of the error on T_i, β_i, l_i, and F_{ai}. Notice that the error on β_i is in fact the error on the momentum p_i, since

$$e_{\beta_i} = \frac{\beta_i(1-\beta_i^2)}{p_i} e_{p_i} .$$

Uncorrelated errors have been assumed, and table 1 gives typical values involved in eq. (10).

By means of eqs. (9) and (10) we can compute the χ^2 of each mass configuration $\mathcal{C}$ as follows:

$$\chi^2_{\mathcal{C}} = \sum_{i=1}^{n} [(g_a)_{i,\mathcal{C}} - \langle g_a \rangle_{\mathcal{C}}]^2/e_i^2 , \quad (11)$$

and identify the configuration giving the minimum $\chi^2_{\mathcal{C}}$ as the best mass assignment for the event. The value of $(\chi^2_{\mathcal{C}})_{\min}$ monitors the quality of the event identification.

From this formulation we derive a natural definition of the probability w for a certain track to be a pion, a kaon, or a proton. This is given by

$$w_i(\pi) = \sum_{\mathcal{C}^*} P_{\mathcal{C}}\,(m_i = m_\pi) / \sum_{\mathcal{C}} P_{\mathcal{C}} , \quad (12)$$

where $P_{\mathcal{C}}$ is the confidence level of $\chi^2_{\mathcal{C}}$ [with $(n-1)$ degrees of freedom] and $\mathcal{C}^*$ is the set of mass configurations in which particle i is assumed to be a pion. Analogous expressions hold true for $w_i(K)$ and $w_i(p)$. From the definition, we obviously obtain that

$$w_i(\pi) + w_i(\mathrm{K}) + w_i(\mathrm{p}) = 1 .$$

Table 1

e_{p_i}	Reconstructed tracks are required to have $e_{p_i}/p_i < 30\%$. The average e_{p_i}/p_i value is $\simeq 3.5\%$.
e_{T_i}	Intrinsic time resolution of the TOF counters, typically about 300 ps.
e_{l_i}	Typically about 1%.
$e_{F_{ai}}$	Typically about 60 ps.

3. Experimental results

Our experiment at the CERN ISR (R415) selected vents with an electron produced at a large angle and dentified by means of Cherenkov and electromag- etic shower counters. Since the latter were placed ehind the TOF counters, the electron time informa- on was always present in our data. Therefore this ack was included in the analysis described above, ıth a fixed mass, i.e. $m(e)$, while the mass assign- ent was operative on all other tracks. Fig. 4 shows e experimental distribution of the $(\chi^2)_{\min}$ confi- nce level P. This distribution is almost flat (as pected for a confidence level distribution), apart om a peak at low-P values which corresponds to ents where no particle identification is possible cause of the presence of accidental wrong-time formation.

The behaviour of the maximum particle identifica- on probability ($w_{\max}$) is shown in fig. 5, $w_{\max}$ being e maximum value between $w(\pi)$, w(K), and w(p) r each track. Notice that owing to its definition, $_{\max} \geqslant \frac{1}{3}$. A peak is present for $w_{\max} \geqslant 0.9$ in the ıree cases, and we have defined as "identified" the

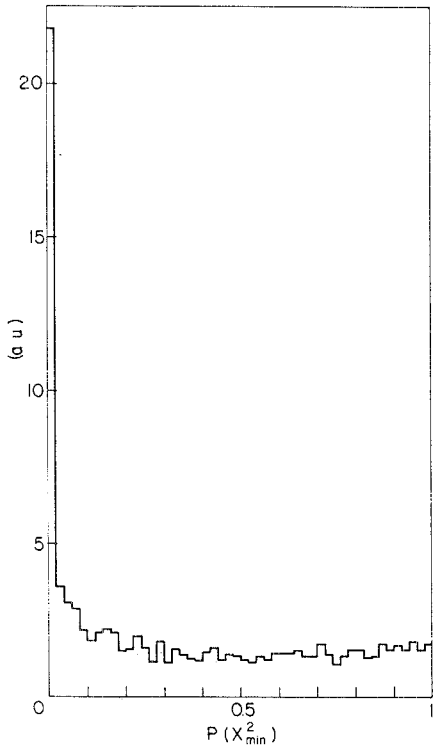

Fig. 4. Distribution of $\chi^2_{\min}$ confidence level obtained with the statistical method.

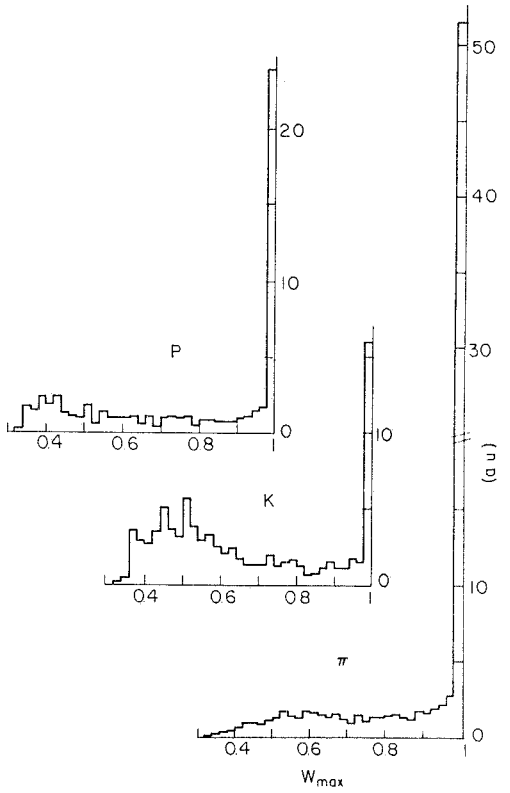

Fig. 5. Distribution of the particle identification maximum probability $w_{\max}$, in the three cases: $w_{\max} = w(\pi)$, $w_{\max} = w$(K), and $w_{\max} = w$(p).

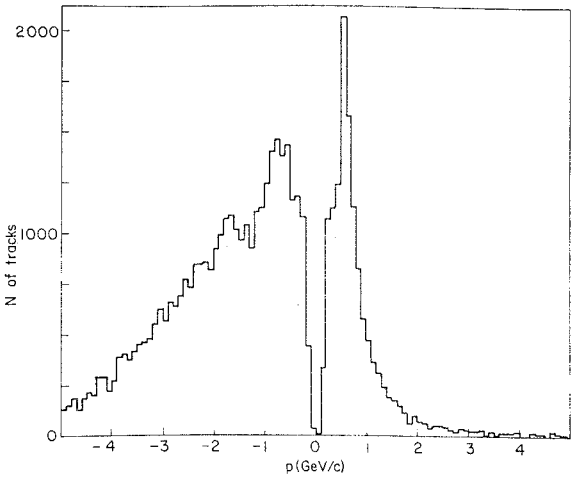

Fig. 6. Momentum distribution of particles produced in pp collisions at $s^{1/2} = 62$ GeV and hitting the TOF counters. Negative momentum values refer to negatively charged particles.

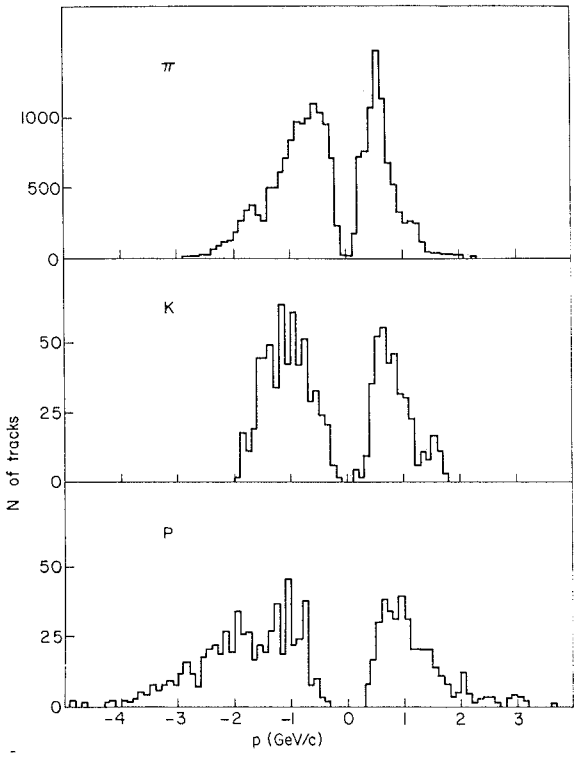

Fig. 7. Same as fig. 6, for particles identified as π, K, or p ($w_{max} \geq 0.9$).

particles belonging to such peaks. The different height of the peaks, relative to π, K, and p, is essentially due to the different yield of these particles in proton–proton interactions [2]. The momentum distribution of the analysed sample of tracks is plotted in fig. 6. This distribution is not symmetrical for positive and negative charge, owing to the acceptance of our apparatus. The amount of identified particles, with $w_{max} \geq 0.9$, turns out to be 50% of this sample.

Figure 7 shows the momentum distribution of identified π, K, and p, which agrees well with the expectations derived from the resolution level of the apparatus (see table 1).

As a cross-check of the validity of our method, we have taken advantage of the presence of the electron trigger track. Since $\beta \simeq 1$ for this track, we can compute the event start-time as follows:

$$g_e = t_s - D_e = (l_e/c) - T_e ,$$

where e is the electron track and counter index, and replace this value in expression (7) to derive the velocity of any other particle:

$$\beta_i = l_i/[c(T_i + g_e + F_{ei})] .$$

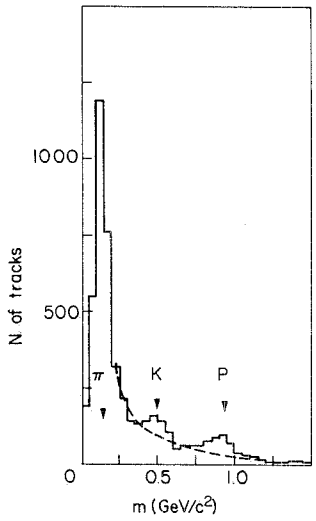

Fig. 8. Mass distribution of particles of all momenta, obtained when using the time information of the trigger electron track only.

Then the mass of the particle can be obtained from its momentum. Fig. 8 shows the particle mass distribution for all momenta. The same distribution is plotted in fig. 9, when the momentum $p < 2.0$ GeV/c; the π contamination in the K and p regions appears to be appreciably reduced. If we now plot the mass obtained in this way for those particles having

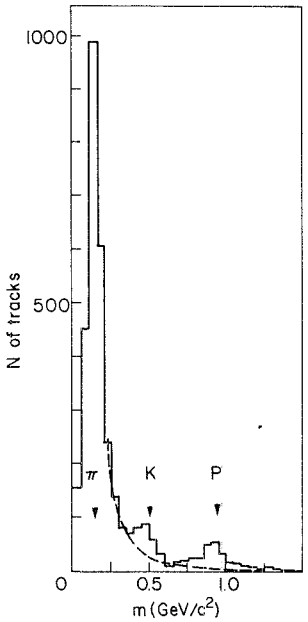

Fig. 9. Same as fig. 8, for particles having momentum $p <$ 2 GeV/c.

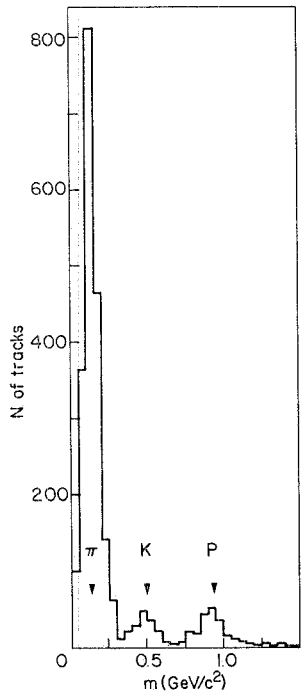

.10. Same as fig. 8, for particles identified by the statisti- method ($w_{max} \geqslant 0.9$).

$_{ax} \geqslant 0.9$, as shown in fig. 10, we see that the con- mination is reduced to a negligible level.

. Monte Carlo and efficiency evaluation

We have performed an accurate Monte Carlo simulation, by means of our real events, using the following procedure:

(a) the charged particles of the event are given the π, K, or p masses according to the known yield of hadrons in proton–proton collisions at 62 GeV total centre-of-mass energy [2]. A good approximation is: 80% of pions, 10% of kaons, and 10% of protons. The trigger track is kept as an electron.

(b) For each track of measured momentum and length (p_i, l_i) and hitting counter C_i, we compute

$$\beta_i = |p_i|/(m_i^2 + p_i^2)^{1/2} ,$$

where m_i is the "Monte Carlo" mass, and the time

$$T_i = (l_i/c\beta_i) + (L_i/2v_i) ,$$

according to expression (7), in the ideal case where the start-time is $t_s = 0$ and $D_i = L_i/2v_i$ (i.e. the delay constants d_i are set to zero). Then we introduce a jitter on T_i by generating a value dT_i from a Gaussian distribution with mean value equal to zero and standard deviation equal to the intrinsic time resolution of counter i (see table 1), and define the time

$$T_i^* = T_i \pm dT_i$$

as the measured time of track i. Analogously, we introduce $p_i^* = p_i \pm dp_i$ and $l_i^* = l_i \pm dl_i$, using in this case the errors e_{p_i} and e_{l_i} relative to the specific track.

(c) We then apply the analysis described so far (in section 2) to our real events in which each track has "simulated" momentum, length, and TOF (p^*, l^*, T^*).

Figure 11 shows the momentum distribution of the identified particles ($w_{max} \geqslant 0.9$), which compares well with the real events distribution of figs. 7. The number of identified particles, compared with the input number of particles, allows evaluation of the efficiency of our analysis for each mass assignment.

The efficiency as a function of the momentum $\epsilon(p)$ for pions, kaons, and protons is shown in fig. 12. Pions are identified up to about 1 GeV/c, kaons up to

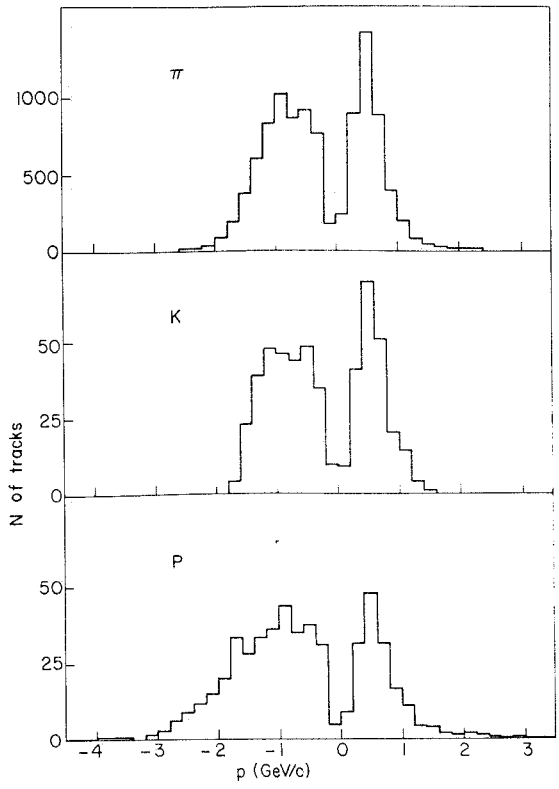

Fig. 11. Same as fig. 7, for Monte Carlo generated tracks.

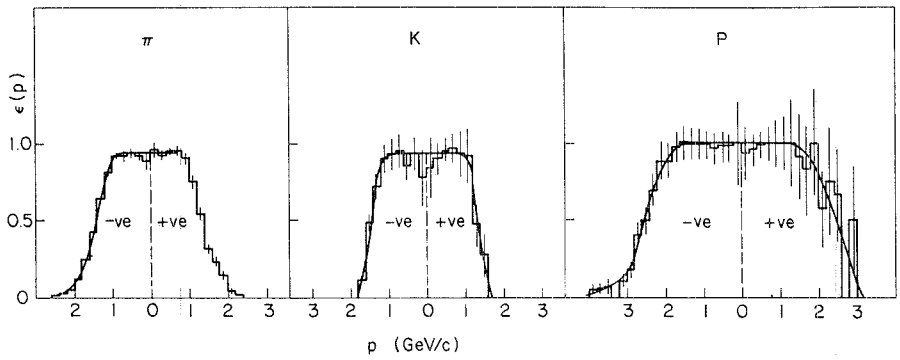

Fig. 12. Particle identification efficiency for π, K, and p, as a function of momentum, shown symmetrically for positive and negative charge.

about 1.4 GeV/c, and protons up to about 2 GeV/c, with efficiency higher than 90%.

The efficiency as a function of the w_{max} cut is shown in fig. 13. With $w_{max} \geq 0.9$, 55% of pions and kaons of all momenta are identified, together with 80% of the protons. Superimposed on the efficiency curve in fig. 13, we have plotted the corresponding contamination curve, i.e. the percentage of erroneously identified tracks. As can be observed, the contamination is nearly zero for pions and protons, and only 10% for kaons when $w_{max} \geq 0.9$. For $w_{max} \geq 0.7$, the contamination for kaons is already 50%, while the efficiency has increased by 10% only. This explains the choice of the cut at 0.9 in the analysis of our data.

Finally, in the Monte Carlo simulation we compare the average start-time distribution ($\langle g_a \rangle$) relative to the minimum χ^2 mass configuration of each event, with the start-time distribution derived from the electron trigger track (see section 3). As can be seen in fig. 14, the standard deviations of these distributions are about 190 ps and about 250 ps, respectively. This again indicates that the statistical method in which all tracks are involved improves the start-time determination accuracy and therefore the identification power of the TOF system.

5. Conclusions

In this paper we have described an efficient method for operating a "non-standard" TOF system in a colliding beam machine (the ISR), taking advantage of the high multiplicity of tracks in the final state to improve the system performance.

Technical developments concerning track mea-

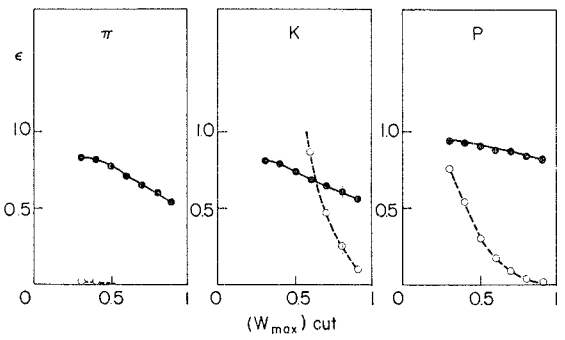

Fug. 13. Particle identification efficiency for π, K, and p, as a function of the cut value applied to w_{max} probability (full-line curve). Superimposed is the contamination curve (dashed-line curve).

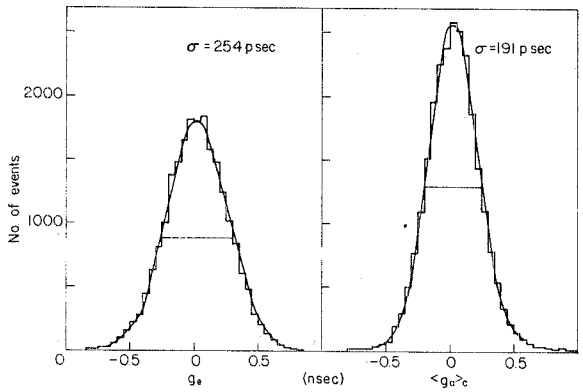

Fig. 14. Distributions of the start-time g_e derived from the trigger electron track and of the average start-time $\langle g_a \rangle_e$, obtained with the statistical method for the minimum χ^2 hypothesis.

surement accuracy and time resolution will push the identification capabilities of such a system even further. Therefore it will be particularly suitable for future colliding beam machines (such as LEP), where the multiplicity will be high and the yield of low-momentum particles still considerable.

Reference

[1] The system of counters was built by the Annecy–CERN–Collège de France–Dortmund–Heidelberg–Warsaw Collaboration.

[2] B. Alper, H. Bøggild, P. Booth, L.J. Carrol, G. von Dardel, G. Damgaard, B. Duff, J.N. Jackson, G. Jarlskog, L. Jöhnsson, A. Kovning, L. Leistam, E. Lillethun, S. Olgaard-Nielsen, M. Prentice and J.M. Weiss, Nucl. Phys. B87 (1975) 19.